J. Agr. Sci. Tech. (2021) Vol. 23(3): 737-749

Hydrodynamic Performance of Triangular Winged Bandal-like Structure in a 180-degree Bend

A. Sardasteh[1], M. Shafai Bejestan[2*], S. A. Ayyoubzadeh [3], and J. M. V. Samani[3]

ABSTRACT

This experiment was conducted in order to determine the hydrodynamic performance of a Triangular Winged Bandal-Like (TWBL) structure, which is a combination of the Bandal-Like (BL) structure and Triangular Vane (TV). For the purposes of this study, the JFE ALEC magnetic velocity meter was used to measure the three components of flow velocity under non-submerged hydraulic conditions at a Froude number of 0.24. The three considered cases for this measurement were the non-structured case and the BL and TWBLs. The results showed that the flow deviation occurred through the impermeable upper part of both structures towards the middle of the channel. At downstream of both structures, bubbling flows were caused by the collision of upward flows with the near-surface flow, causing disturbances in the latter. Both the BL and the TWBL structure reduced the secondary flow strength along the bend within the structure range. Compared to the BL structure, the TWBL structure reduced the secondary flow strength by about 20%, which indicates the weaker inclination of the secondary flow toward the outer bank in the TWBL structure. The relative maximum shear stress in the TWBL structure is on average 17% lower than that of the BL structure.

Keywords: Flow pattern, Karun river, Meandering river, Secondary flow strength, Shear stress.

INTRODUCTION

River bend migration is a common phenomenon that causes substantial irreparable damage to the surrounding areas in meandering rivers. A field study conducted in the Karun River, the largest river in Iran, has reported a maximum migration rate of 884 meters from 1991 to 2007 (Morshedi and Alavi Panah, 2010). This has been the result of developing a secondary flow at the river bend resulting in scouring the toe of the outer river bank and creation of point bars at the inner river bank (Odgaard and Bergs, 1988). In the past, extensive flow-altering measures have been introduced including spurs (Zhang *et al*., 2012), submerged vanes (Odgaard and Spoljaric, 1986; Odgaard and Wang, 1991; Odgaard, 2009;), bendway weirs (Derrick, 1996; Davinroy *et al*., 1998; Abad and Rhoalds, 2008; Jia *et al*., 2009; Jarrahzade and Shafai-Bejestan, 2011; Cunningham and Lyn, 2016), W-weir (Bhuiyan, *et al*. 2007, 2009); cross-vanes (Endreny and Soulman, 2011; Pagliara and Mahmoudi-Kurdistani, 2013), and the implementation of a bubble screen across the flow (Dugue *et al*. 2013). The high sedimentation rate, especially during the flood period between the spurs, has led to the use of the Impermeable Spur Dike (ISD) for bank stabilizing and controlling the river bend migration as well as rectifying the navigable rivers (Copeland, 1983; Carling *et al*., 1996; Shields *et al*., 2003). To reduce the construction cost in deep meandering rivers, Bandal-Like (BL) structures have been studied as an option. This structure consists of two parts: the upper impermeable

[1] Khuzestan Water and Power Authority Company, Ahvaz, Islamic Republic of Iran.
[2] Department of Water Structures, Shahid Chamran University of Ahvaz, Ahvaz, Islamic Republic of Iran.
[*] Corresponding author; e-mail: m_shafai@yahoo.com
[3] Department of Water Structures, Tarbiat Modares University, Tehran, Islamic Republic of Iran.

[DOR: 20.1001.1.16807073.2021.23.3.7.4]

part and the lower permeable part (Rahman *et al*., 2003a, b, 2005, 2006; Teraguchi, 2011; Teraguchi *et al*. 2011b; Nakagawa *et al*., 2011; Zhang *et al*., 2013). Studies have proven that the BL structure can modify the flow pattern along the bend to prevent scouring of the outer bank. However, for the restoration of the outer bank, the flow vortex that causes sedimentation in between the two structures is too weak. Triangular vane is an environmental flow-altering structure extensively studied by Bhuiyan *et al*. (2010) in a sine-generated flume and Bahrami-Yarahmadi and Shafai-Bajestan (2016) in a 90-degree flume bend. The results of these studies show that the flow overspilling the crest of the vane creates a counter-clockwise secondary flow in the outer bank, counteracting the clockwise main secondary flow cell of the bend. In the downstream sections of the vane, the downwelling zone, located between two secondary flow cells and the core of maximum depth-averaged velocity, is shifted to the middle of the flume and the size of counterclockwise secondary flow cell is increased. The average size of the counterclockwise secondary flow cell was about 30 percent of the flume width. Such a flow pattern can result in transportation of sediment over the vane toward the outer bank. To improve the performance of BL structure, Sardasteh *et al*. (2017) proposed a modification to this structure type to increase the rate of deposition in between the structures as well as the depth of the scour hole. The new structure is a combination of BL and Triangular Vane (TV) structures and is called Triangular Winged Bandal-Like (TWBL) structure. The purpose was to incorporate the advantages of both the BL and TV structures. Sardasteh *et al*. (2020) conducted an experimental study on the characteristics of bed surrounding in the TWBL, BL and ISD structures in a 180° flume. The experiments were carried out at a Froude number of 0.24 and a constant flow depth of 12 cm. The effective Length (L) of all structures was 14 cm. All tests were conducted under clear water conditions and in the turbulent flow range. A total of 9 different alternatives of the TWBL structure, three different ratios of the effective Length of the BL part (L_b) to the effective Length of structure (L) ($L_w = L_b/L$), and three different TV part angles (α= 20, 30, 50 degrees) with respect to the upstream bank were each tested at a Froude number of 0.24. The results showed that the case with $L_w = 0.64$ and α=50° scored the first rank. The maximum relative scour depth and the relative volume of the scour hole of the TWBL structure were calculated to be 31% and 54% smaller than those of the ISD structure, respectively. The relative deposition height for the TWBL structure was found to be higher than that of the ISD and BL structures for all flow conditions with increases of 47 and 96%, respectively. Moreover, the relative length of deposition in the TWBL structure was higher than that of the ISD and the BL structures by 55 and 386%, respectively. In the TWBL structure, the sediments accumulated behind the structure along and near the outer bank, forming a deposition shape with a larger length and better form.

As shown, the flow pattern in the BL structure has been rarely addressed and, similarly, there is a lack of study on the TWBL structure in the literature. Hence, this study was conducted in order to better understand the hydrodynamic changes caused by installation of BL and TWBL structures in 180-degree bends as well as the changes in the velocity pattern and shear stress distribution. Thus, the aim of this study was to further explore the function of TWBL as a countermeasure for toe bank erosion through laboratory experiments.

MATERIALS AND METHODS

Experimental Setup

A total of 14 tests were conducted in a 180-degree flume in the hydraulic laboratory of the Shahid Chamran University of Ahvaz as shown in Figure 1. Uniform sand with a

[DOR: 20.1001.1.16807073.2021.23.3.7.4]

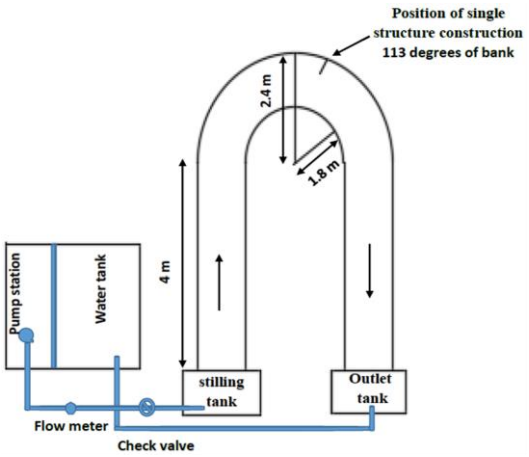

Figure 1. Experimental setup of 180-degree flume.

relative density of 2.63 and median size of 0.88 mm was used.

The experiments were carried out for the BL and TWBL structures and the non-structural case, at the flow rate of 18.7 L s^{-1}, the mean flow Velocity (V) of 26 cm s^{-1} and the corresponding Froude number of 0.24 at a constant flow depth of 12 cm. The threshold velocity of sediment movement (Vc) was measured to be 0.307 m/s. Therefore the velocity ratio (V/Vc) is equal to 0.85 which is less than one, thus all tests were carried out at clear water conditions. The corresponding Reynolds number was equal to 31,200, ensuring a fully turbulent flow.

The WBL structures, as shown in Figure 2-a, were constructed by attaching a TV structure, made of Plexiglas with a thickness of 5 mm, to the head of a BL structure. The effective length of the WBL structure (i.e. the sum of effective lengths of the BL and TV structures) was 14cm (≤ 30% of the flume width as recommended by DHI (1992) and Perdok (2002). In all of the structures, the height of the impermeable and permeable sections of the BL structure was half the depth of the flow (Teraguchi, 2011). In the BL structure, Figure 2-b, the lower half of the structure was made of metal wire with a diameter of 5 mm and a permeability of 50% (Teraguchi *et al*., 2011b; Zhang *et al*., 2013), and the impermeable upper part was made of Plexiglas with a thickness of 5 mm.

The initial experiment was conducted on the ISD without attaching the triangular vane. The experiment lasted for 13 hours at a Froude number of 0.24, where almost 90% of the maximum scour depth occurred in the first 150 minutes. Therefore, considering the fact that the aim of this study was to compare different alternative structures and not developing criteria for bed scouring, a duration of 180 minutes was considered for all the tests. In addition, by performing preliminary tests, an angular position of 113 degree was determined to install the structures on the 180-degree bend. In this

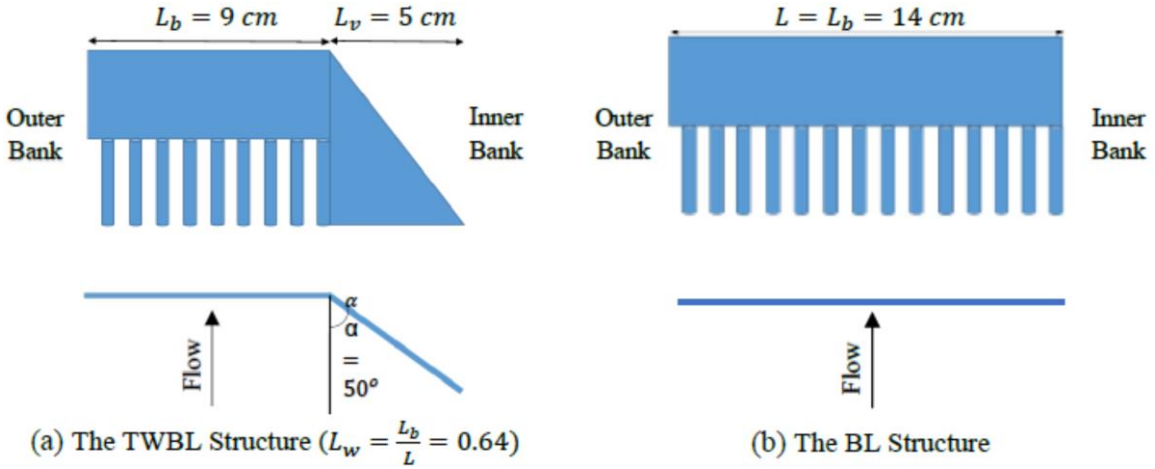

Figure 2. The triangular winged Bandal-like (TWBL) and The Bandal-like (BL) structures.

[DOR: 20.1001.1.16807073.2021.23.3.7.4]

position, the largest scour dimension occurred, which was also consistent with that suggested in other studies (Rozovskii, 1957).

For each test, first, the structure (BL or TWBL) was installed at the outer bank of flume at the position of 113 degree. As shown in Figure 1, each test was started by flattening the bed, starting the pump and allowing water to gradually enter the flume whilst the tailgate is completely closed. Once the flow depth reached a sufficient level, the entrance valve was gradually opened at the same time with the tail gate until the desired flow discharge and flow depth were achieved. These conditions were maintained until the change in scour depth, which was measured at a half hour interval by a point gage, was slowed down to less than one mm per hour. The pump was then shut down and the flume was gradually drained. The scour surface was then fixed by using cement powder, small enough to cause the stick particles and scour bed profiles unchanged, and prepare it for measurement of 3D velocity components.

3D Flow Velocities Measurements

The three-Dimensional (3D) velocity components were measured using the electromagnetic velocity meter JFE ALEC model ACM3-RS. The accuracy of the measurement by the device was 2% or 0.5 cm s^{-1} with a resolution of 0.1 cm s^{-1}. The rate of data capture by this device is between 15 and 60 Hz. At the bottom of the metal stem of the speedometer was a detector that measured the three-dimensional velocity components at each point by creating an electromagnetic field around it. Output data was stored in RAW format, which can convert registered data to CSV format through WinLabEM (software provided by device maker) and can be read with Excel software. The sampling rate was 20 Hz and a minimum sampling duration of 90 seconds was selected. Thus, a total of 1,800 pieces of data were collected for each point, the mean value of which was used for analysis of the 3D flow pattern. The measurement was conducted in a total of 560 nodes at 8 cross-sections, namely, 107-, 110-, 112-, 114-, 116-, 119-, 124- and 134-degree sections from the bend inlet. In each cross-section, 14 vertical lines with lateral distances of 3, 5.5, 8, 10.5, 13, 15.5, 18, 20.5, 24, 30, 36, 42, 48 and 54 cm from the outer bank were

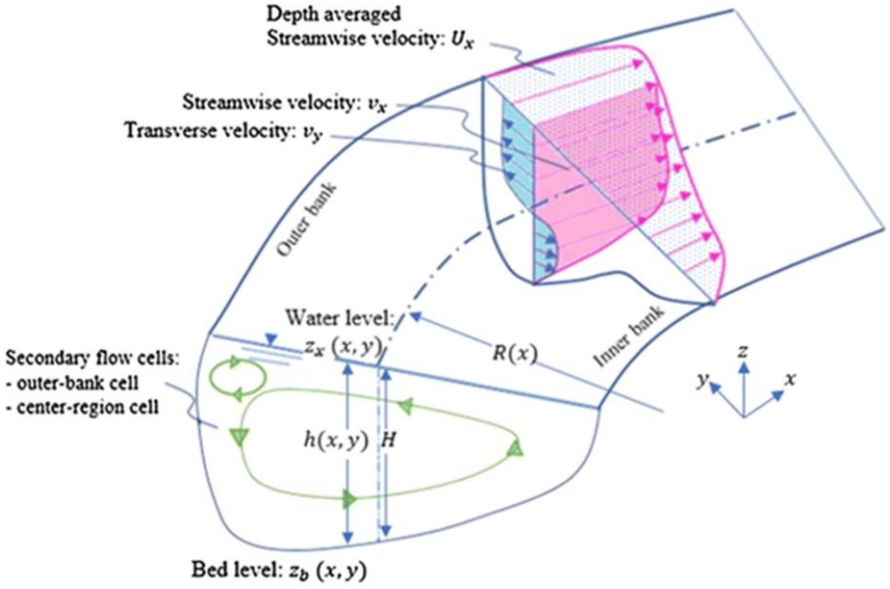

Figure 3. 3D flow velocities and the secondary flow in the bend (Shaheed *et al*., 2019)

[DOR: 20.1001.1.16807073.2021.23.3.7.4]

selected. At each vertical line, the minimum number of the points for recording the 3D velocity components was 5 (3, 5, 7, 9 and 11 cm above the bed). Figure 3 shows 3D flow velocities in the bend.

Bed Shear Stress

The sediment pattern along the bends depends on the distribution of shear stress (Dietrich *et al*., 1979; Rahman *et al*., 1998). In order to better understand the effect of the structure on sediment management in the bend, the shear stress distribution is needed to be studied. To this end, the depth-averaged two-dimensional hydrodynamic equations were used for calculation of the bed shear stress measurement data (Kilanehei *et al*., 2011; Ahmadi *et al*., 2009; Wu, 2007; Duan and Nanda; 2006; Hsieh and Yang, 2003; Kassem and Chaudhry, 2002).

$$\tau_{bx} = \rho C_f u\sqrt{u^2 + v^2} \quad (1)$$

$$\tau_{by} = \rho C_f v\sqrt{u^2 + v^2} \quad (2)$$

$$\tau_b = \sqrt{{\tau_{bx}}^2 + {\tau_{by}}^2} \quad (3)$$

$$C_f = \frac{g}{C^2} = \frac{gn^2}{h^{\frac{1}{3}}} \quad (4)$$

Where, u and v are, respectively, the mean velocity (m s^{-1}) along the x and y directions, τ_{bx} and τ_{by} are, respectively, the bed shear stresses (N m^{-2}) along the x and y directions, τ_b is the resultant bed shear stress (N m^{-2}), ρ is the density of the fluid, g is the gravity coefficient, C_f is non-dimensional Chezy's coefficient, n is Manning coefficient, and h is the depth of flow.

Secondary Flow Strength

As shown in Figure 3, the secondary flow, i.e. the movement of the surface layers towards the outer bend and the lower layers to the inner bend, is the most important factor in the change in the distribution of shear stress and thus the distribution pattern of the deposit in the bends. The strength of this secondary flow affects the bed shear stress and, therefore, studying this strength and its changes in presence of a structure is important. In other words, the secondary flow strength expresses the flow tendency for deviation to the outer bank in the curved paths. By conducting studies on flow in the river bend, Shukry (1950) defined the strength of secondary flows as follows:

$$S_{xy} = \frac{K_{lateral}}{K_{main}} = \frac{\sum(v_i^2 + w_i^2)\Delta A_i}{\sum(u_i^2 + v_i^2 + w_i^2)\Delta A_i} \quad (5)$$

Where, S_{xy} is the Strength of the secondary flow, u_i, v_i, and w_i are the longitudinal, transverse, and vertical components of velocity in the cells of the section, respectively, and ΔA_i is the cross-sectional Area of each of the cells. In a given transverse section, this criterion is defined as the ratio of the kinetic energy of the transverse flow to that of the main flow.

RESULTS AND DISCUSSION

Velocity Distribution

The streamlines along the surface water for the BL and TWBL structures are shown in (Figure 4 a-b), respectively. The flow deviation occurred through the impermeable upper part of both structures towards the middle of the channel. At downstream of both structures, bubbling flows are caused by the collision of upward flows with the near-surface flow, causing disturbances in the latter. In the BL structure, the bubbling flow moved towards the structure at low velocities and along the back-side alignment of the blockage plate towards the main channel. The diverted flow from the back-side is preventing the recirculation currents in this region. The field velocity in the BL structure is attenuated after passing through the structure, but the magnitude of the velocity vectors is increased along the main channel. This finding is consistent with the results reported by Teraguchi *et al*. (2011b), Nakagawa *et al*. (2011), and Zhang *et al*. (2013). In the TWBL structure, the bubbling flow moved towards downstream at a low

[DOR: 20.1001.1.16807073.2021.23.3.7.4]

velocity. The flow of scouring sediments in the direction of the triangular plate moved towards the outer bank, which was effective in increasing the sediment deposited near the outer bank. At downstream of the triangular vane, part of the velocity vectors moved towards the structure, and a counterclockwise vortex was formed behind the upper part (impermeable region), continuing its path towards the downstream.

Figure 4-a shows that flow (at high velocities) is diverted towards the main channel and the inner bank. Figure 4-b shows the velocity vectors (at low velocities) at the downstream of the structures and near the outer bank, consequently, causing deposition in this region.

Bed Shear Stress

The results of the calculations (bed shear stress distribution pattern) at cross-sections of 107, 110, 112, 114, 116, 119, 124 and 134 degrees and a cross-section of the straight path of the bend are shown in (Figure 5-a, b and c) for the non-structured case and the BL and TWBL structures, respectively. For the non-structural case, it is observed that in the second half of the bend, the shear stresses were gradually transferred from the middle of the channel to the outer bank. The maximum stresses occur near the outer bank, which is also consistent with the field tests. It is also observed that a smaller share of the stresses is distributed in the vicinity of the inner bank compared to the outer bank, which is due to the presence of centrifugal forces in the bend and the transfer of higher-velocity flows to the outer bank.

For the BL and TWBL structures, due to the deviation of the surface layers through the upper impermeable part of the structure towards the middle of the channel, larger stresses are distributed at the middle of the channel section. However, due to the permeability of the lower part of the structure and the possibility of passing of the flows in the lower layers, the flow velocity behind the structure is reduced, causing a smaller portion of the stress to be distributed near the outer bank.

In both structures, the shear stress in the scour hole experiences an increase and the largest shear stress occurs at the bottom of the scour hole, which is consistent with the research by Dietrich *et al*. (1979). However, compared to the BL structure, the amount of the maximum shear stress and its extent are lower in the TWBL structure, which in turn prevents occurrence of scouring unlike the

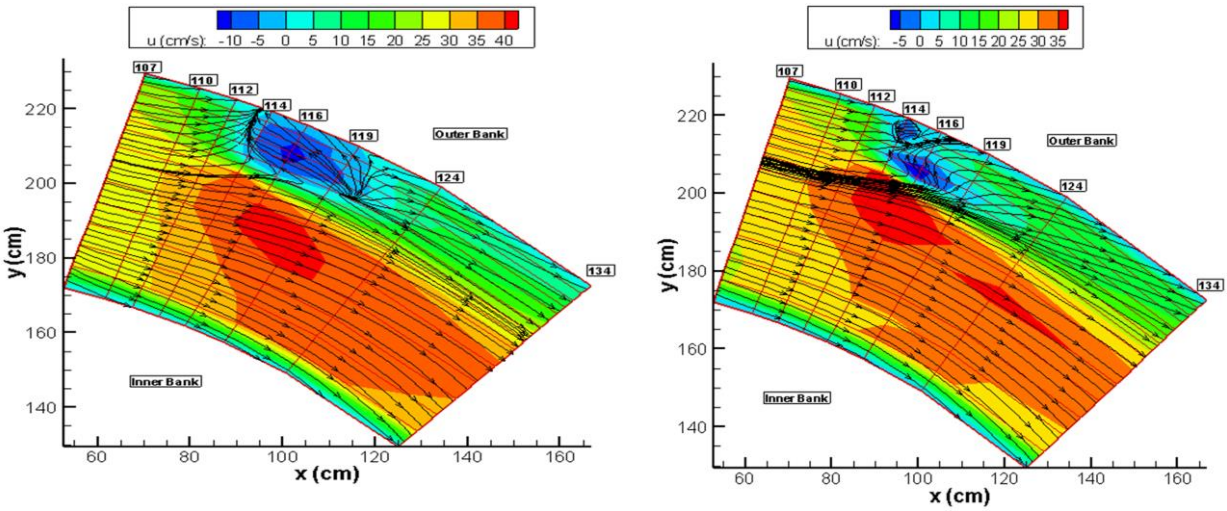

(a) (b)

Figure 4. The streamlines on the water surface and longitudinal velocity contour(a) (BL), (b)(TWBL).

[DOR: 20.1001.1.16807073.2021.23.3.7.4]

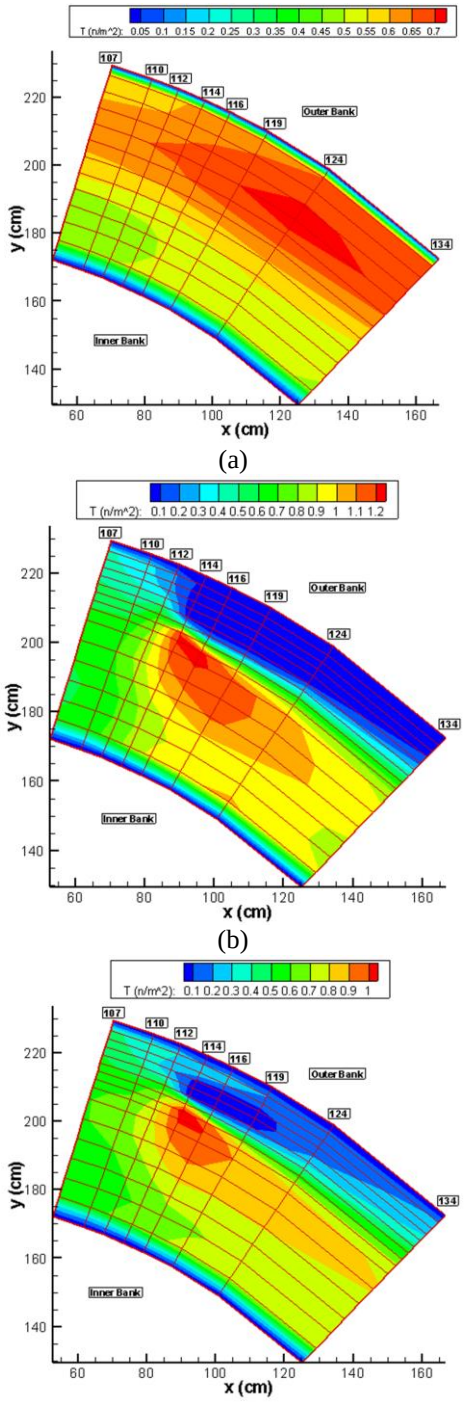

Figure 5. Shear stress distribution pattern a): (non-structured), b): (BL), and c): (TWBL)

BL structure. The largest depth of the scouring and its extent occurred before the installation of the structure compared to the BL structure.

According to some researches, the secondary flow in the channel bends causes a large shear force compared to the straight path, meaning that the bed shear stress analysis is more complicated in the bend compared to the straight path (Smith and McLean, 1984). In order to investigate the maximum relative shear stress variations in the upstream and down-stream of a single-structure position, the ratio of the maximum shear stress in the bend to the shear stress at the straight part was calculated. The reason for this is the higher efficiency of secondary flows in the bend compared to that of the straight path as well as the high shear force generated due to the existence of these flows (Smith and McLean, 1984).

For the non-structural case, as shown in Figure 9, the maximum relative shear stress is higher than 1, which indicates that the shear stress in the bend is greater than that in the straight path, confirming the results reported by Smith and McLean (1984). The difference between the minimum and maximum relative shear stresses in the non-structured case is about 13%, which represents the roughly uniform distribution of the relative maximum shear stress in the non-structured case in the upstream and downstream regions of the single-structure position.

As shown in Figures 10 and 11, for both the BL and the TWBL structures, the relative maximum shear stress is greater than 1. It can be seen that by approaching the position at which the structure is installed, the shear stress is increased relative to the non-structured case, which is due to the narrowing of the flow duct and the subsequent increase in velocity and flow per unit width. Table 1 shows the variations of relative maximum shear stress for the three cases. The maximum relative shear stress are increased by 56 and 30%, respectively, relative to the non-structured case. The relative maximum shear stress for the TWBL structure is, on the average, 17% lower than that of the BL structure.

[DOR: 20.1001.1.16807073.2021.23.3.7.4]

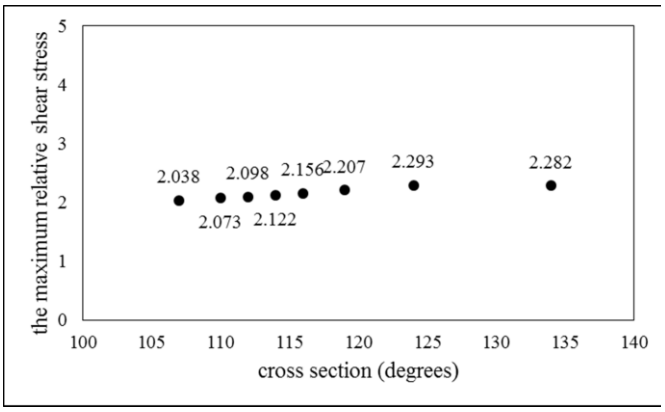

(a)

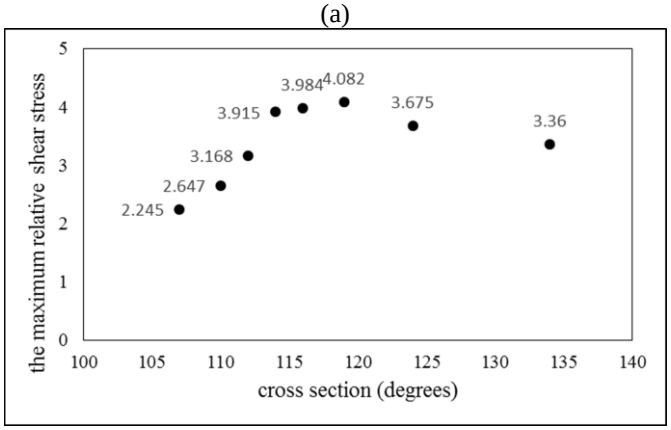

(b)

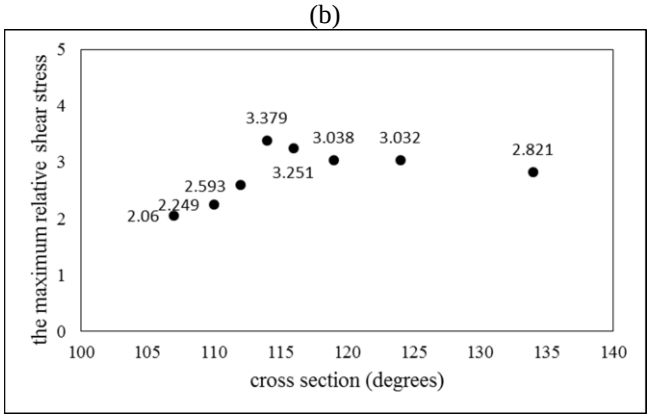

(c)

Figure 9. Variation of the maximum relative shear stress a): (non-structured), b): (BL), and c): (TWBL)

Table 1. The relative maximum shear stress variations.

Cross-section	BL to NS	TWBL to NS	TWBL to BL
107 °	10	1	-8
110 °	28	8	-15
112 °	51	24	-18
114 °	84	59	-14
116 °	85	51	-18
119 °	85	38	-26
124 °	60	32	-17
134 °	47	24	-16

[DOR: 20.1001.1.16807073.2021.23.3.7.4]

Compared to the BL structure, the scouring and its extent occurred before the installation of the structure in the TWBL structure.

Secondary Flow Strength

In this section, Equation (5) was used to calculate the secondary flow strength in Sections 107 to 134 and plot the changes. Figures 12, 13, and 14 show the variation of the secondary flow strength along the bend in the upstream and downstream of the single-structure position for non-structured, BL, and TWBL cases. As seen for the non-structured case, the distance between the positions of 107° and 134° along the bend is

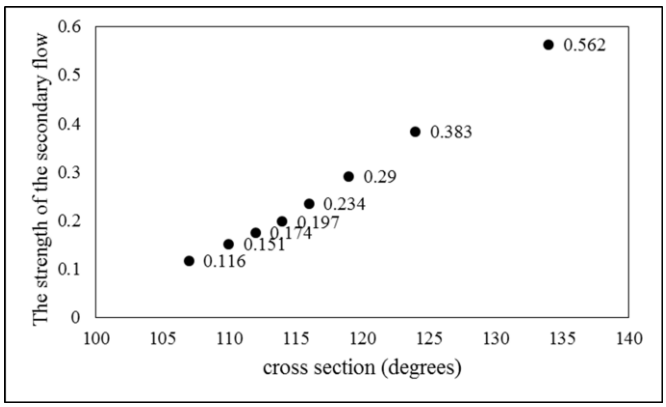

(a)

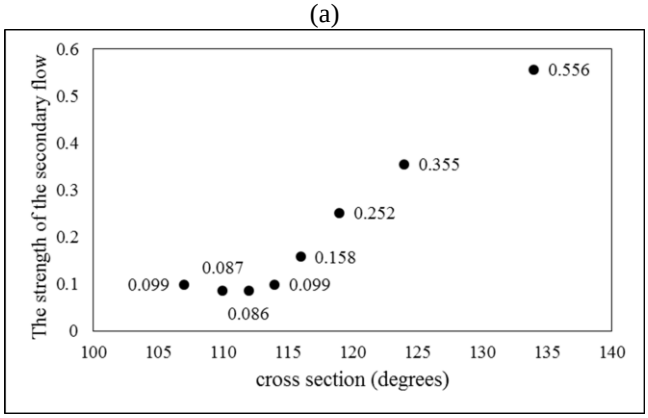

(b)

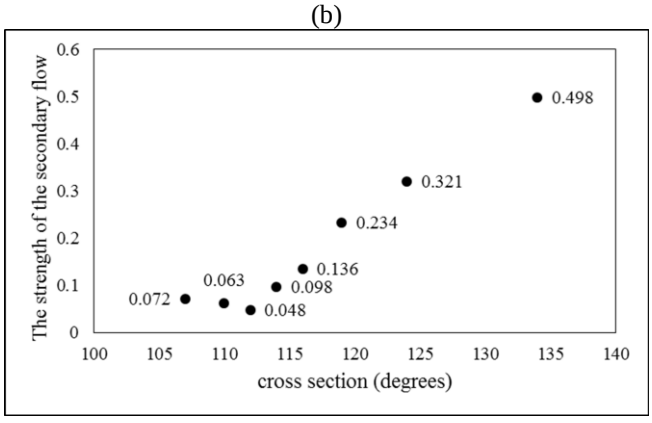

(c)

Figure 9. Variation of the secondary flow strength a): (non-structured), b): (BL), and c): (TWBL)

[DOR: 20.1001.1.16807073.2021.23.3.7.4]

Table 2. The secondary flow strength variations. of

Cross-section	BL to NS	TWBL to NS	TWBL to BL
107 °	-15	-38	-27
110 °	-42	-58	-28
112 °	-51	-72	-44
114 °	-50	-50	-1
116 °	-32	-42	-14
119 °	-13	-19	-7
124 °	-7	-16	-10
134 °	-1	-11	-10

ascendingly increased. This is due to the collision of the flow with the outer bank, as well as the increase in the square of the transverse velocities and the reduction of the square of the longitudinal velocities.

By comparing Figures 13 and 14 with Figure 12, it can be concluded that the presence of the BL and the TWBL structures reduces the secondary flow strength along the bend in the upstream and downstream range of the single-structure position. Table 2 shows the strength variations of the secondary flow for the considered three cases. Compared to the non-structured case, the BL and TWBL structures reduce the secondary flow strength by about 26 and 38%, respectively. Compared to the BL structure, the TWBL structure reduces the secondary flow strength by about 20%, which indicates the lower inclination of the secondary flow toward the outer bank in the TWBL structure.

CONCLUSIONS

The flow deviation occurred through the impermeable upper part of both structures towards the middle of the channel. At the downstream of both structures, bubbling flows are formed by collision of upward flows with near-surface flows, ultimately causing disturbances in the latter. Both the BL and the TWBL structures reduced the strength of the secondary flow along the bend within the structure range. The TWBL structure, compared to the BL structure, reduces the secondary flow power by about 20%, which indicates the lower inclination the secondary flow toward the outer bank in the TWBL structure. Therefore, in this structure, the outer bank protection, deposition, and coastal development are better than the BL structure. The relative maximum shear stress in the TWBL structure is, on the average, 17% lower than that of the BL structure. Compared to the BL structure, the scouring and its extent occurred before the installation of the structure in the TWBL structure.

ACKNOWLEDGEMENTS

The authors would like to appreciate Tarbiat Modares University for its supports in this research as a part of the first author PhD thesis and the Faculty of Water Engineering of Shahid Chamran University of Ahvaz for its support and the Khuzestan Water and Power Authority Company and the Khuzestan Water and Power Authority Company to use its Internet and the library.

REFERENCES

1. Abad, J. D. and Rhoalds, B. L. 2008. Flow Structure at Different Stages in a Meander-Bend with Bendway Weirs. *J. Hydraul. Eng.*, **134(8):** 1052-1063.
2. Ahmadi, M. M., Ayyoubzadeh, S. A., Montazeri Namin, M. and Mohammad Vali Samani, J. 2009. A 2D Numerical Depth-Averaged Model for Unsteady Flow in Open Channel Bends. *J. Agr. Sci. Tech.,* 1**1:** 457-468.
3. Bahrami Yarahmadi, M. and Shafai Bajestan, M. 2016. Sediment Management

[DOR: 20.1001.1.16807073.2021.23.3.7.4]

and Flow Patterns at River Bend Due to Triangular Vanes Attached to the Bank. *J. Hydro-Environ. Res.,* **10**: 64–75.
4. Bhuiyan, F., Hey, R. D. and Wormleaton, P. R. 2007. River Restoration Using W-Weir. *J. Hydraul. Eng.*, **133(6):** 596–609.
5. Bhuiyan, F., Hey, R. D. and Wormleaton, P. R. 2009. Effects of Vanes and Weirs on Sediment Transport in Meandering Channels. *J. Hydraul. Eng.,* **135(5):** 339–349.
6. Bhuiyan, F., Hey, R. D. and Wormleaton, P. R. 2010. Bank-Attached Vanes for Bank Erosion Control and Restoration of River Meanders. *J. Hydraul. Eng.,* **136(9):** 583-596.
7. Carling, P. A., Kohmann, F. and Gols, E. 1996. River Hydraulics, Sediment Transport and Training Works: Their Ecological Relevance to European Rivers. *Archiv. Hydrobiol. Suppl.,* **113(10):** 129-146.
8. Copeland, R. R. 1983. *Bank Protection Techniques Using Spur Dikes*. Hydraulics Laboratory, US Army Corps of Engineers, Waterways Experiment Station, Vicksburg, Mississippi.
9. Cunningham, R. and Lyn, D. 2016. Laboratory Study of Bendway Weirs as a Bank Erosion Countermeasure. *J. Hydraul. Eng.*, https://doi:10.1061/(ASCE) HY.1943-7900.0001117, 04016004.
10. Davinroy, R. D., Rapp, R. J. and Myhre, R. E. 1998. Hydroacoustic Study of Fishes in Bendway Weir Fields of the Middle Mississippi River. *Proc., Wetlands Engineering and River Restoration Conf.*, ASCE, Reston, VA, PP.890–895.
11. Derrick, D. L. 1996. The bendway weir: An in-Stream Erosion Control and Habitat Improvement Structures for the 1990's. *Proc., XXVII Int. Conf. on Erosion Control Technology-Bringing Home*, Erosion Control Association, Steamboat Springs, Colo., PP. 227–241.
12. DHI. 1992. Hydraulic Manual of Mike 11 Mode, a Microcomputer Based Modelling System for Rivers and Channels. Danish Hydraulic Institute (DHI). Denmark.
13. Dietrich, W. E., Smith J. D. and Dunne, T. 1979. Flow and Sediment Transport in a Sand Bedded Meander. *J. Geol.,* **87**: 305-315.
14. Duan, J. G. and Nanda, S. K. 2006. Two-Dimensional Depth-Averaged Model Ssimulation of Suspended Sediment Concentration Distribution in a Groyne Field. *J. Hydrol.,* **327:** 426– 437.
15. Dugue, V., Blanckaert, K., Chen, Q. and Schleiss, A. J. 2013. Reduction of Bend Scour with an Air-Bubble Screen-Morphology and Flow Patterns. *Int. J. Sediment Res.,* **28(1):** 15–23.
16. Endreny, T. A. and Soulman, M. M. 2011. Hydraulic Analysis of River Training Cross-Vanes as Part of Post-Restoration Monitoring, *Hydrol. Earth Syst. Sci.,* **15:** 2119-2126.
17. Hsieh, T. Y. and Yang, J. C. 2003. Investigation on the Suitability of Two–Dimensional Depth-Averaged Models for Bend-Flow Simulation. *J. Hydraul. Eng. ASCE,* **129(8):** 597- 612.
18. Jarrahzade, F., and Shafai-Bejestan, M. 2011. Comparison of Maximum Scours Depth in Bank Line and Nose of Submerged Weirs in a Sharp Bend. *Sci. Res. Essays*, **6(5):** 1071-1076.
19. Jia, Y., Scott S., Xu, Y., and Wang, S. S. Y. 2009. Numerical Study of Flow Affected by Bendway Weirs in Victoria Bendway, the Mississippi River. *J. Hydraul. Eng. ASCE*, **135(11):** 902-916.
20. Kassem, A. A. and Chaudhry, F. 2002. Numerical Modelling of Bed Evolution in Channel Bends. *J. Hydraul. Eng. ASCE*, **128(5):** 507-514.
21. Kilanehei, F., Naeeni, S. T. O. and Namin, M. M. 2011. Coupling of 2DH-3D Hydrodynamic Numerical Models for Simulating Flow around River Hydraulic Structures. *World Appl. Sci. J.,* **15(1):** 63-77.
22. Morshedi, J. and Alavi Panah, S. K. 2010. Change Prediction of Karoon River Lengths by Using Historical and Quantitative Geomorphologic Data (From Shoshtar to Arvandrod). *Quarterly Geographic. J. Territory*, **6(22):** 43-58.
23. Nakagawa, H., Teraguchi, H., Kawaike, K., Baba, Y. and Zhang, H. 2011. Analysis of Bed Variation Around Bandal-Like Structures. *Annuals of Disas. Prev. Res. Inst., Kyoto University,* **54B:** 497- 510.
24. Odgaard, A. J. and Spoljaric, A. 1986. Sediment Control by Submerged Vanes. *J. Hydraul. Eng.,* **112(12):** 1164.
25. Odgaard, A. J., and Bergs, M. A. 1988. Flow Processes in a Curved Alluvial Channel. Water Resour. Res., **24 (1)**: 45-56.
26. Odgaard, A. J. and Wang, Y. 1991. Sediment Management with Submerged

[DOR: 20.1001.1.16807073.2021.23.3.7.4]

Vanes. I: Theory. *J. Hydraul. Eng.*, **117(3):** 267–283.
27. Odgaard, A. J. 2009. River Training and Sediment Management with Submerged Vanes. ASCE Press, 184 PP.
28. Pagliara, S. and Mahmoudi Kurdistani, S. 2013. Scour Downstream of Cross-Vane Structures, *J. Hydro-Environ. Res.*, **7(12):** 236–242.
29. Perdok, U. H. 2002. *Application of Timber Groynes in Coastal Engineering.* MSc. Thesis, TU Delft University of Technology.
30. Rahman, M. M., Nagata, N. and Muramoto, Y. 1998. Effect of Side Slope on Flow and Scouring Around Spur-Dike-Like Structures. Proc., 7th Int. Symp. on River Sedimentation, Hong Kong, China, 165-171.
31. Rahman, M. M., Nakagawa, H., Ishigaki, T. and Khaleduzzaman, A. T. M. 2003a. Channel Stabilization Using Bandalling. *Annual of Disaster Prevention Research Institute, Kyoto University*, **46B**: 613-618.
32. Rahman, M. M., Nakagawa, H., Khaleduzzaman, A. T. M. and Ishigaki, T. 2003b. Flow and scour-deposition around bandals. *Proceeding Fifth International Summer Symposium*, Japan Society of Civil Engineers, Tokyo, Japan.
33. Rahman, M. M., Nakagawa, H., Khaleduzzaman, A. T. M., and Ishigaki, T. 2005. Formation of the Navigational Channel Using Bandal-Like Structures. *Ann. J. Hydraul. Eng. Japan Society of Civil Engineers*, **49:** 997-1002.
34. Rahman, M. M., Nakagawa, H., Ito, N., Haque, A., Islam, T., Rahman, M. R., and Hoque, M. M. 2006. Prediction of Local Scour Depth around Bandal-Like Structures. *Ann. J. Hydraul. Eng. Japan Society of Civil Engineers*, **50:** 163-168.
35. Rozovskii, I. L. 1957. *Flow of Water in Bends of Open Channels.* Published by the Academy of Sci. Ukrainian SSR, Kiev.
36. Sardasteh, A., Ayyoubzadeh, S. A., Shafai Bajestan, M. and Mohammad Vali Samani, J. 2017. Introduction of Winged Bandal-like Structure and Comparison of Bed Topography Changes to Bandal-Like and Impermeable Spur Dyke Structures at a 180-Degree Bend in Non-Submerged Conditions. *16 the Iranian Hydraulic Conference*, Ardabil, Iran.
37. Sardasteh, A., Ayyoubzadeh, S. A., Shafai Bajestan, M. and Mohammad Vali Samani, J. 2020. River Bed Sediment Management by the Winged Bandal-Like Structure and Selection of Optimum Structure Using Ranking of SAW and TOPSIS Methods. *Iranian J. Sci. Technol., Transactions Civil Engin*. **44**: 1373-1383.
38. Shaheed, R., Mohammadian, A. and Kheirkhah Gildeh, H. 2019. A Comparison of Standard k–ε and Realizable k–ε Turbulence Models in Curved and Confluent Channels. *Environ. Fluid Mech.*, 19: 543-568.
39. Shields, F. D., Copeland, R. R., Klingeman, P. C., Doyle, M. W. and Simon, A. 2003. Design for Stream Restoration. *J. Hydraul. Eng.*, **129(8):** 575-584.
40. Shukry, A. 1950. Flow around Bends in an Open Flume. *Trans. Am. Soc. Civil Eng.*, **115(1):** 751-779.
41. Smith, J. D. and Mclean, S. R. 1984. A Model for Flow in Meandering Streams. *Water Resour. Res.*, **20(9):** 1301-1315.
42. Teraguchi, H. 2011. Study on Hydraulic and Morphological Characteristics of River Channel. PhD Thesis, Kyoto University Research Information Repository, 146 PP.
43. Teraguchi, H., Nakagawa, H., Kawaike, K., Baba, Y. and Zhang, H. 2011b. An Alternative Method for River Training Works Bandal-Like Structures. *Ann. J. Hydraul. Eng. Japan Soc. Civil Eng.*, **55:** 151-156.
44. Wu, W. 2007. *Computational River Dynamics.* Taylor & Francis/Balkema Publisher, National Center for Computational HydroScience and Engineering, University of Mississippi, MS, USA.
45. Zhang, H., Nakagawa, H., Ogura, M. and Mizutani, H. 2012. Bed Morphology and Grain Size Characteristics around a Spur Dyke. *Int. J. Sediment Res.*, **27(2):** 141-157.
46. Zhang, H., Nakagawa, H., Ogura, M. and Mizutani, H. 2013. Experiment Study on Channel Bed Characteristics around Spur Dykes of Different Shapes. *Int. J. Sediment Res.*, **28:** 489-499.

[DOR: 20.1001.1.16807073.2021.23.3.7.4]

عملکرد هیدرودینامیکی سازه باندال لایک باله مثلثی در قوس ۱۸۰ درجه

ع. سردسته، م. شفاعی بجستان، س. ع. ایوب زاده، و ج. م. و. سامانی

چکیده

این مطالعه تجربی به منظور تعیین عملکرد هیدرودینامیکی سازه باندال لایک باله مثلثی انجام شده، که ترکیبی از سازه باندال لایک و صفحه مثلثی می باشد. برای انجام این مطالعه، از سرعت سنج مغناطیسی JFE ALEC برای اندازه گیری سه مؤلفه سرعت جریان در شرایط هیدرولیکی غیر مستغرق در عدد فرود ۰/۲۴ استفاده شد. برای این اندازه گیری، سه حالت بدون سازه، سازه باندال لایک و سازه باندال لایک باله مثلثی در نظر گرفته شده بود. نتایج نشان داد که انحراف جریان از طریق قسمت فوقانی غیرقابل نفوذ هر دو سازه به سمت وسط کانال رخ داده است. در پایین دست هر دو سازه، برخورد جریان های رو به بالا با جریان نزدیک سطح، جریان های جوشان را ناشی شده که باعث تلاطم می شوند. هر دو سازه باندال لایک و باندال لایک باله مثلثی قدرت جریان ثانویه را در طول قوس داخل محدوده سازه کاهش می دهند. سازه باندال لایک باله مثلثی در مقایسه با سازه باندال لایک، قدرت جریان ثانویه را حدود ۲۰٪ کاهش می دهد، که نشان دهنده تمایل کمتر جریان ثانویه به سمت دیواره بیرونی در سازه باندال لایک باله مثلثی می باشد. حداکثر تنش برشی نسبی در سازه باندال لایک باله مثلثی به طور متوسط ۱۷٪ کمتر از سازه باندال لایک است.

[DOR: 20.1001.1.16807073.2021.23.3.7.4]